

# Calcium phosphate formation on plasma immersion ion implanted low density polyethylene and polytetrafluorethylene surfaces

Alexey Kondyurin · Emilia Pecheva ·  
Lilyana Pramatarova

Received: 27 April 2006 / Accepted: 5 July 2007 / Published online: 15 August 2007  
© Springer Science+Business Media, LLC 2007

**Abstract** The flexible structure of polymers has enabled them to be useful in a wide variety of medical applications due to the possibility to tailor their properties to suit desired applications. For a long time, there has been an increasing interest in utilizing polymers as matrices for calcium phosphate-based composites with applications in hard tissue implants. On the other side, polymers with application as heart valves, urea catheters and artificial vessels present a case where the formation of minerals (namely calcification) should be avoided. The modification of polymer surfaces by various ion beam treatments for reducing the calcification, as for example plasma immersion ion implantation (PIII), is well known and has a long time effect. This work is part of a wider investigation of the ability of plasma immersion ion implanted polymers to induce calcium phosphate formation from an aqueous solution resembling the human blood plasma. In the experiment described in this paper, topographical and chemical changes were inserted on the surfaces of two conventional polymers (low density polyethylene and polytetrafluorethylene) by PIII with nitrogen ions, and under conditions mimicking the natural mineral formation processes. The effect of the plasma modification on the calcium phosphate nucleation and growth from the aqueous solution was ambiguous. We suppose that the complex combination of surface characteristics influenced the

ability of the plasma treated polymer films to induce the formation of a calcium phosphate layer.

## 1 Introduction

Ion beam implantation (IBI) is known as a method for controlled and selective surface modification of polymer materials without altering their bulk properties. Modified polymer surfaces find specific applications in the human body as heart valves, artificial vessels, urea catheters, mammary, face and finger prosthesis [1–5]. Among IBI, plasma immersion ion implantation (PIII) is frequently used to convert hydrophobic polymers to hydrophilic. This process can also improve the adhesion strength, biocompatibility, and other pertinent properties, as well as to change a polymer hydrophilic behavior to hydrophobic [1, 6–8]. It is known that three processes take place when a material (polymer or other) is introduced into a living organism, where the ambient media are generally aqueous solutions. These are: rapid protein absorption as monolayers on the surfaces, cell attachment [9–12] and mineralization of the surface [12]. Mineralization in nature is a process involving complex interactions between inorganic ions, crystals and organic molecules in an aqueous media. The organic and inorganic counterparts are continuously interacting with each other and the result is the formation of mineralized tissues with convoluted architecture and distinguished microscopic design [13–16]. In the case of polymers introduced into a living organism as soft tissue implants, the biomineralization process, including the formation of calcium or calcium phosphate deposits, on their surface is not desired. For example, calcium deposits or protein layers formed on the internal

---

A. Kondyurin  
School of Physics, A28, University of Sydney, Sydney, NSW,  
Australia  
e-mail: a.kondyurin@physics.usyd.edu.au

E. Pecheva (✉) · L. Pramatarova  
Institute of Solid State Physics, Bulgarian Academy of Sciences,  
72, Tzarigradsko Chausee blvd., Sofia 1784, Bulgaria  
e-mail: emily@issp.bas.bg

sides of artificial vessels can obstruct the blood circulation; calcification can decrease the elasticity of soft tissue implants like mammary prosthesis, which brings pain to the patient and limits the implant life-time. Heart valve operations can be unsuccessful after time due to calcification of the valve walls which make them non-elastic [4, 17, 18]. Therefore, the prevention of the mineralization on the polymer surfaces in the body is attributed to the success of some medical polymer implants.

This work is part of a wider investigation of the ability of PIII treated polymers (low density polyethylene, polytetrafluorethylene, 2103 and 2363 commercial Pelletane materials with medical applications and polyurethane synthesized from polypropyleneglycol and toluenediisocyanate, PPG-TDI) to induce calcium phosphate formation from an aqueous solution resembling the human blood plasma. In this paper we study the modification of two conventional polymers, low density polyethylene and polytetrafluorethylene, by PIII with nitrogen ions, and their ability for calcium phosphate formation after the modification upon immersion in an aqueous solution of inorganic salts. This approach was chosen because it mimics the natural mineral formation processes.

## 2 Experiment

### 2.1 Polymer samples

Low density polyethylene (LDPE; Goodfellow, England) and polytetrafluorethylene (PTFE; Halogen, Russia) films with thickness of 50 and 20  $\mu\text{m}$ , respectively, were used in the experiments. The surface of the films was cleaned by distilled water, alcohol and acetone, and air dried before surface modification.

### 2.2 Surface modification

LDPE and PTFE films were modified by PIII with various doses of 20 keV nitrogen ions ( $5 \times 10^{14}$ ,  $5 \times 10^{15}$ ,  $2 \times 10^{16}$  and  $5 \times 10^{16}$  ions/cm<sup>2</sup>). Doses were varied by the pulse frequency. The depth of the modified layer on LDPE and PTFE surfaces at 20 keV nitrogen ion implantation is equal to 90 nm according to calculations with TRIM code. Sample holder had additional electrode and a metal grid that excluded direct contact of samples with radio frequency plasma between the high voltage pulses and also avoided charging effect during high voltage pulse. The grid was placed on 40 mm distance over the polymer films which excluded shadow effect on the modified surfaces. Residual atmosphere and working pressure of nitrogen at PIII were  $1 \times 10^{-3}$  and  $5 \times 10^{-1}$  Pa,

respectively. Other conditions of PIII were 5  $\mu\text{s}$  pulse duration, 200 W plasma power, 13.56 MHz radio frequency plasma, and full time in plasma discharge of 10 min for all doses. Pulse repetition frequency from 0.2 Hz to 100 Hz was used to exclude overheating during the PIII treatment. Non-implanted films were used as control samples.

### 2.3 Calcium phosphate growth

The ability of the modified polymer films to induce calcium phosphate formation was tested by their immersion in a supersaturated solution resembling the human blood plasma—simulated body fluid (SBF) for 4 h at 37 °C. Two base solutions were prepared by reagent-grade chemicals. The first one consisted of NaCl (15.99 g/L), KCl (0.45 g/L), CaCl<sub>2</sub> · 2H<sub>2</sub>O (0.74 g/L) and MgCl<sub>2</sub> · 6 H<sub>2</sub>O (0.61 g/L) dissolved in 1 L of distilled water. The second one included Na<sub>2</sub>SO<sub>4</sub> · 10H<sub>2</sub>O (0.32 g/L), NaHCO<sub>3</sub> (0.71 g/L) and K<sub>2</sub>HPO<sub>4</sub> · 3H<sub>2</sub>O (0.69 g/L) dissolved in 1 L of distilled water. The pH of the two solutions was buffered at 7.4 with tris-hydroxymethyl-aminomethane buffer (CH<sub>2</sub>OH)<sub>3</sub>CNH<sub>2</sub>) or hydrochloric acid. Before immersion of the samples, equal quantities of the two base solutions were mixed to obtain the final SBF solution. The ion concentrations of the SBF presented in Table 1 are compared to the concentrations of the human blood plasma [19].

### 2.4 Surface analysis

The analysis of the polymer films and of the effect of the ion doses on the calcium phosphate formation was examined by contact angle measurements, AFM, optical microscopy, FTIR in ATR and transmission modes, and micro-Raman spectroscopy.

The surface wettability of the polymer films after PIII and before layer growth was studied by a contact angle measuring system DSA10 (Kruss, Germany) with water drops and by using the method of sessile drop. The contact angle was determined by analysis of the drop geometry through video-imaging and calculation by Rabel approximation model of water drop form.

**Table 1** Ion concentrations of the human blood plasma and the SBF used for calcium phosphate growth on the polymers films

Ion concentrations (mM)							
	Na <sup>+</sup>	K <sup>+</sup>	Mg <sup>2+</sup>	Ca <sup>2+</sup>	Cl <sup>-</sup>	HCO <sub>3</sub> <sup>-</sup>	HPO <sub>4</sub> <sup>2-</sup>
Plasma	142.0	5.0	1.5	2.5	103.0	27.0	1.0
SBF	142.0	5.0	1.5	3.75	148.8	4.2	1.5

AFM observations were carried out on DMA scanning probe optical microscope DualScope C-21 in tapping mode under ambient conditions.

FTIR transmission spectra were recorded on Nicolet Magna 750 spectrometer, using 100 scans and resolution of  $2\text{ cm}^{-1}$ . FTIR ATR spectra were recorded with ZnSe crystal in ATR accessory and angle of light beam accident  $45^\circ$ . Spectra were analyzed by OMNIC Nicolet software.

Micro-Raman spectra were obtained in a backscattering mode ( $\lambda = 532,14\text{ nm}$ ) on diffraction double monochromator spectrometer HR800, Jobin Yvon, LabRam System 010. Spectral resolution was  $4\text{ cm}^{-1}$ . Number of scans and integration time were varied for sufficient signal-to-noise ratio. Optical microscope Olympus BX40 with objectives of  $50\times$  and  $100\times$  was used for imaging of the surfaces. LabRam software was used for spectra analysis.

Optical microscope Nikon Eclipse ME600 with magnification objectives of  $5\times$ ,  $20\times$  and  $50\times$  was used to observe the topography of the polymer films before and after their immersion in the SBF. Digital video camera was used for microphoto image recording.

### 3 Results and discussion

In vivo synthetic materials are subjected to the influence of various body liquids that are generally aqueous (blood, urine, and etc.). Wettability is perhaps the most important surface parameter that determines the quantity and quality of adsorbed proteins and materials biocompatibility [20]. For that reason we investigated the wettability properties of the LDPE and PTFE films before their immersion in the SBF and the change of their surface contact angle with water, in relation to the treatment with PIII. The results for the measured contact angle  $\theta$  are presented in Table 2 and show high value for the non-implanted LDPE and PTFE films (controls:  $92.8^\circ$  and  $112.4^\circ$ , respectively), i.e. these surfaces were hydrophobic and they were expected to be poorly wettable by body liquids. It is generally known that PTFE has low surface adhesion which prevents coatings from adhering to its surface [21–23]. After the application of the PIII treatment with doses  $1 \times 10^{14}$  and  $1 \times 10^{15}\text{ cm}^{-2}$  on the LDPE films, the contact angle strongly decreased to  $56.8^\circ$ – $58.3^\circ$  (see Table 2) which

make the LDPE amenable to good adhesion. However, with the highest dose ( $1 \times 10^{16}\text{ cm}^{-2}$ ) the contact angle increased again, reaching  $78.3^\circ$ . The same tendency for decreased contact angle after the PIII with doses of  $1 \times 10^{14}$  and  $1 \times 10^{15}\text{ cm}^{-2}$  (from  $112.4^\circ$  to  $81.2^\circ$ – $97.5^\circ$ ) and significant increase with the highest dose ( $126.9^\circ$  at  $1 \times 10^{16}\text{ cm}^{-2}$ ; strongly hydrophobic surface) was observed for the PTFE films (Table 2).

Observation with AFM showed that the topography of the smooth polymer films was changed to surfaces with increased surface area after the PIII treatment (Fig. 1). The topography change for LDPE had a character of wrinkling of the surface layer. The reason for this topography change is in the internal stresses appearing in the modified surface layer which were subsequently relaxed due to movement to the bulk of the polymer. Similar changes were previously

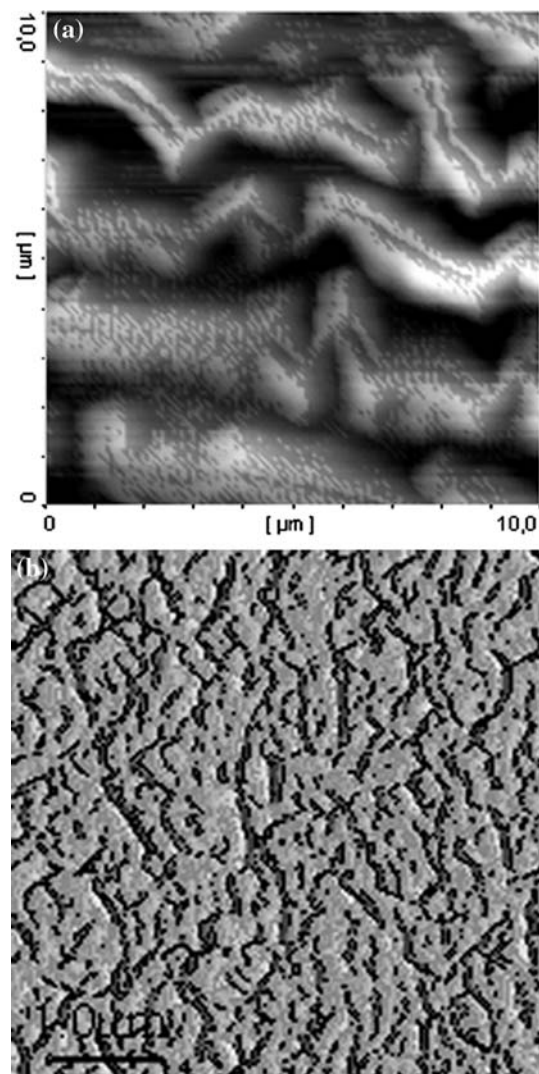


**Fig. 1** AFM shows the topography changes of the smooth polymer films after the PIII modification: (a) LDPE, (b) PTFE

**Table 2** Change of the wettability properties (contact angle  $\theta$ ,  $^\circ$ ) of the LDPE and PTFE films with the PIII doses

Doses of PIII ( $\text{N}^+/\text{cm}^2$ )	Control	$1 \times 10^{14}$	$1 \times 10^{15}$	$1 \times 10^{16}$
LDPE	$92.8 \pm 2.0^\circ$	$56.8 \pm 5.1^\circ$	$58.3 \pm 7.7^\circ$	$78.3 \pm 3.1^\circ$
PTFE	$112.4 \pm 0.3^\circ$	$97.5 \pm 0.3^\circ$	$81.2 \pm 5.5^\circ$	$126.9 \pm 0.1^\circ$

observed in studies of other types of polymers [24]. The surface topography change for PTFE had a characteristic of etching of the surface layer [25].

The surface structure of the control and modified LDPE and PTFE films was analyzed by FTIR in ATR mode (Fig. 2). The spectra of untreated LDPE (Fig. 2a, spectrum 1) showed the characteristic C–H vibrational modes of polyethylene macromolecules, i.e. rocking, bending and stretching modes at  $719/729\text{ cm}^{-1}$  (doublet),  $1463/1473\text{ cm}^{-1}$  (doublet) and  $2800\text{--}3000\text{ cm}^{-1}$ , respectively [26]. Lines with weaker intensity at  $883$  and  $887\text{ cm}^{-1}$  (unsaturated out-of-plane C–H group vibrations), and two distinguished regions at  $990\text{--}1210\text{ cm}^{-1}$  (C–O stretching vibrations in ether, ester, alcohol) and  $1660\text{--}1770\text{ cm}^{-1}$  (C=O stretching modes of carbonyl, carboxyl, ketone, aldehyde, ether and ester groups) were also observed. Other oxygen containing group line was observed as a broad peak centered at  $3400\text{ cm}^{-1}$  (hydroxyl) and probably O–H scissoring mode was present as a narrow peak at  $1640\text{ cm}^{-1}$ . Unsaturated C=C groups in hydrocarbon-containing compounds were detected as modes at  $1300$  and  $1600\text{--}1630\text{ cm}^{-1}$  in the spectrum of LDPE control sample. Oxygen-containing and double carbon-carbon groups on the LDPE surface appeared due to ageing processes in the polymer. Aromatic ring breath vibrations were found at  $1597\text{ cm}^{-1}$  due to the presence of antioxidant in the LDPE film. The low intensity of these lines corresponded to a low concentration of the defected macromolecule in the untreated LDPE film.

FTIR ATR spectra of the modified LDPE films (Fig. 2a, spectra 2–5) revealed significantly increased intensity of the C–O, C=O, C=C and O–H stretching vibrations (the regions at  $980\text{--}1260\text{ cm}^{-1}$ ,  $1660\text{--}1780\text{ cm}^{-1}$ ,  $1600\text{--}1630\text{ cm}^{-1}$  and  $3120\text{--}3700\text{ cm}^{-1}$ , respectively). This result

shows that the concentration of the hydrophilic groups (C–O, C=O, and O–H) was increased. In addition, lines at  $910$  and  $966\text{ cm}^{-1}$  due to unsaturated C–H groups (vinyl and vinylene) appeared which correspond to the presence of end-groups of polyethylene macromolecules as a result of polymerization process from ethylene. The increased content of oxygen-containing and double carbon-carbon groups was assigned to the PIII treatment which has broken polymer chains and made the surfaces highly reactive through the energetic ion bombardment. Subsequently, chemical reactions between the unstable reactive radicals, and oxygen and carbon from the air took place, resulting in stronger oxidation of the top surface (increased concentration of surface hydrophilic functional groups, such as C=O, C–O and O–H) under storage in air after the PIII treatment and carbonization of the underlying surface layers [21, 27].

FTIR ATR spectra of the control PTFE film (Fig. 2b, spectrum 1) revealed basic C–F stretching modes of fluoroethylene macromolecules as very strong lines at  $620/640$  (doublet) and in the region of  $1100\text{--}1300\text{ cm}^{-1}$ . C–O and C=O stretching modes were present with very low intensity in the regions of  $830\text{--}970$  and  $1600\text{--}1800\text{ cm}^{-1}$ . Very weak lines were also observed at  $1420$ ,  $1459$  and  $1599\text{ cm}^{-1}$  as bending vibrations due to hydrocarbon traces. In the spectra of the PIII modified PTFE films (spectra 2–5), the lines due to oxygen-containing groups (C=O stretching modes in carbonyl, carboxyl, ketone, aldehyde, ether and ester) appeared in the region  $1600\text{--}1810\text{ cm}^{-1}$  with increased intensity which means that the concentration of the hydrophilic groups becomes higher. Stretching due to unsaturated C=C groups was also detected in this region. These features reflect oxidation and carbonization processes in the PTFE in a similar manner to the LDPE surface, increased under the energetic bombardment [21, 27].

Optical microscopy in reflection mode was used for observation of the polymer films after their immersion in the SBF aqueous solution. Pyramidal crystals grouped in dendrite formations were covering the surfaces, with different density and crystal dimensions (Fig. 3). According to our previous studies where pyramidal crystals were observed on various surfaces, they were identified as NaCl crystals by using energy dispersive X-ray spectroscopy analysis [28–30]. This result could mean that the modified films became more susceptible to water absorption since it is known that the presence of sodium ions on polymer surfaces increases the absorption of water in aqueous medium [31].

Figures 4 and 5 show the optical images of LDPE and PTFE controls and plasma treated films. In addition to the dendrites, white crystals were observed covering the surfaces heterogeneously. The number of the crystals changed

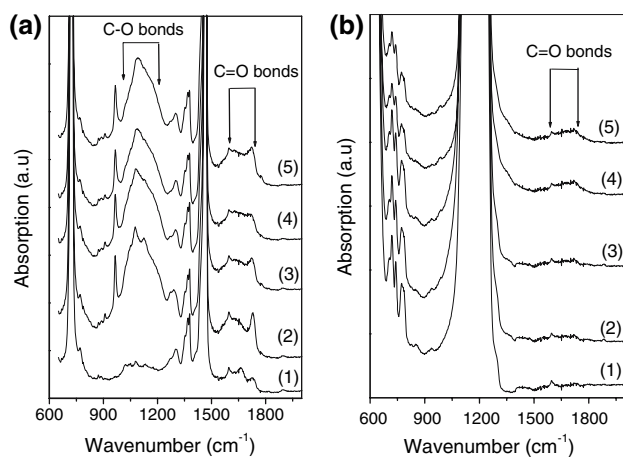


**Fig. 2** FTIR ATR spectra of (a) LDPE and (b) PTFE after PIII modification with nitrogen ions: (1) control sample, (2)–(5) films implanted with doses of  $5 \times 10^{14}$ ,  $5 \times 10^{15}$ ,  $2 \times 10^{16}$  and  $5 \times 10^{16}\text{ cm}^{-2}$

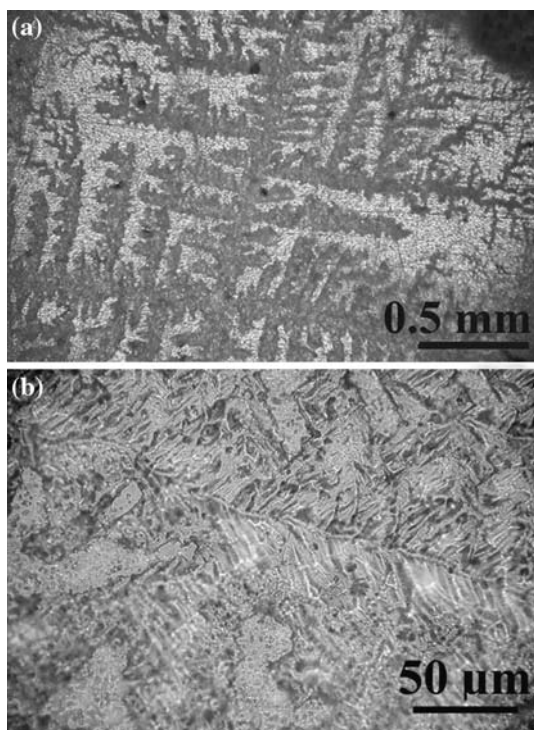


**Fig. 3** Optical microscope images of the polymer films after the layer deposition from SBF: (a) magnification  $\times 5$  and (b)  $\times 50$

with the dose of the ion implantation. It was observed that the concentration of the white crystals increased with increasing the dose of PIII for both polymers. The dimensions of the pyramidal crystals followed the same tendency—the biggest crystals were observed on the films implanted with the higher doses. The PTFE control also yielded high density of white crystals. All PTFE samples, modified and control, showed higher concentration of these crystals in respect to the LDPE samples, although the much higher contact angle of PTFE suggested lower wettability and hence lower layer adhesion.

The structure of the two types of polymers after the PIII modification and immersion in the SBF for 4 h was analyzed with FTIR spectroscopy in transmission mode (Fig. 6a). The spectra showed the formation of specific functional groups on the surface of LDPE and PTFE. The vibrations observed at  $719/729\text{ cm}^{-1}$  (doublet),  $1463/1473\text{ cm}^{-1}$  (doublet) and  $2800\text{--}3000\text{ cm}^{-1}$  were characteristic of C–H vibrational modes of  $\text{CH}_2$  and  $\text{CH}_3$  groups in LDPE (rocking, bending and stretching modes, respectively). According to Fig. 6b, the C–F vibrational modes in the spectra of PTFE were detected at  $514, 554, 627/640$  (doublet) and  $1100\text{--}1300\text{ cm}^{-1}$ , as typical bending and stretching modes of  $\text{CF}_2$  and  $\text{CF}_3$  groups [26]. After the immersion of the polymers in the SBF, a small shoulder at  $1050\text{ cm}^{-1}$  was found in the spectra due to contribution of the  $\nu_3$  P–O asymmetric stretching mode, characteristic of

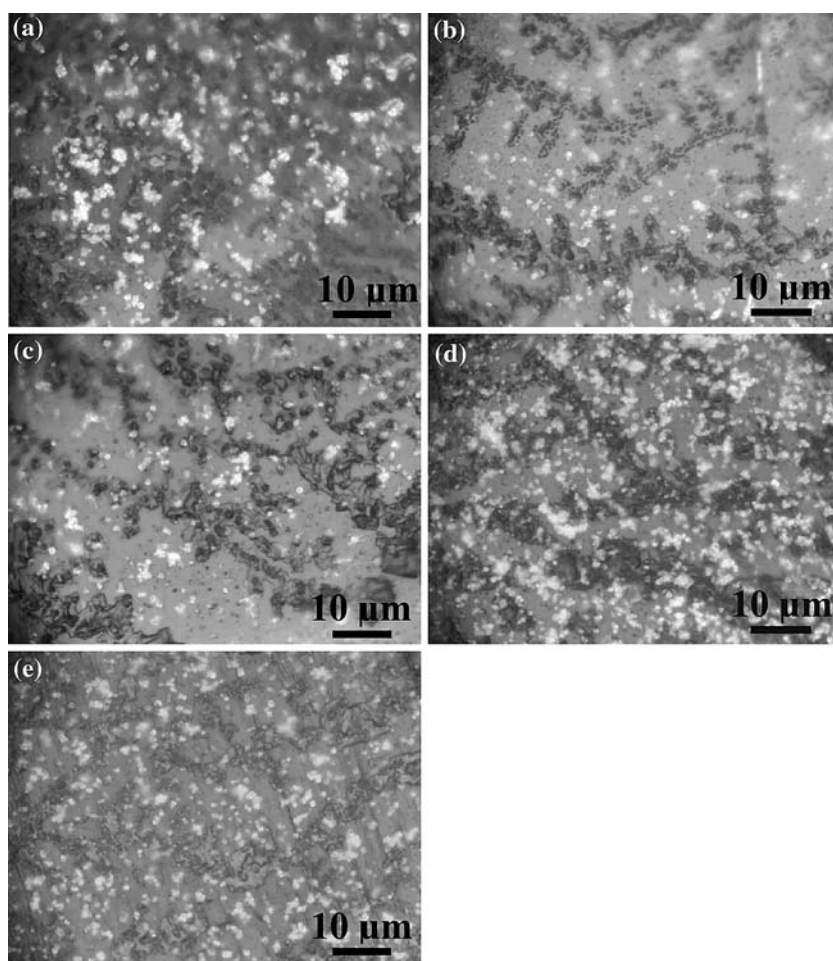
calcium phosphates ( $\text{PO}_4$ ). This shows that calcium phosphate layer was grown on the control and PIII treated LDPE and PTFE films from the supersaturated aqueous solution. Calculation of the relative layer thickness was carried out based on the obtained FTIR results. As known from the Beer's law for the light propagating through an absorbing material with thickness  $z$ , the optical density of the layer is related proportionally to its thickness following the dependence:

$$I = I_{\text{IN}} \cdot e^{-\alpha z},$$

where  $I$  is the intensity of the light passing through the layer,  $I_{\text{IN}}$  is the light incident intensity,  $\alpha$  is the absorption coefficient of the layer [32]. In this experiment, the optical density of the grown calcium phosphate layers was calculated for the control and treated LDPE and PTFE polymers, and Fig. 7 depicts the results for the absorption line at  $\nu = 1050\text{ cm}^{-1}$ . No clear dependence of the layer thickness in relation to the application of PIII treatment and increase of doses was observed. The same results were obtained after the calculation of the optical density at other wavenumbers ( $1636, 1710$  and  $1736\text{ cm}^{-1}$ ). This implies that either the calcium phosphate formation of the modified surfaces was not dependent on the PIII treatment or simply the duration of the samples immersion in the SBF (4 h) was too short to observe a difference.

Micro-Raman spectroscopy was also used in this work as a complimentary technique to the FTIR spectroscopy which is more powerful when thin layer need to be analyzed, as in our experiment. Focusing on the crystals in the layer was possible due to the micrometer size of the beam and allowed us to collect more signal from the layer with minimum influence of the underlying polymer films. Figure 8 shows the recorded Raman signal for control LDPE and PTFE films (spectrum 1), controls after the growth of the layer from SBF (spectrum 2), as well as the PIII treated films after the growth of the layer (treated with a dose of  $2 \times 10^{16}\text{ N}^+/\text{cm}^2$ ; spectrum 3). Strong peaks observed at  $1061.7, 1129.1, 1295.6, 1417.6, 1440.3$  and  $1460.4\text{ cm}^{-1}$  in Fig. 8a, spectrum 1 were due to the characteristic C–C and C–H bands in the LDPE control sample [26, 33]. After its immersion in the SBF for 4 h, additional peaks at  $428.5, 561.2$  and  $954.4\text{ cm}^{-1}$  were present as seen in spectrum 2. They were assigned to  $\nu_2$  asymmetric bending,  $\nu_4$  symmetric bending and  $\nu_1$  symmetric stretching vibrations of  $\text{PO}_4$  in calcium phosphate. Generally,  $\nu_1$  stretching mode is the strongest peak in the spectrum and it is very narrow, thus indicating good crystallinity [34]. The broad peak in our spectrum was ascribed to the lower degree of crystallinity of our layer which has not matured. It is known that at precipitation from aqueous solution, before the final formation of crystalline hydroxyapatite, other precursor

**Fig. 4** Optical microscope images of LDPE control and plasma treated films after the calcium phosphate deposition: (a) control, (b)  $5 \times 10^{14}$  ions/cm<sup>2</sup>, (c)  $5 \times 10^{15}$  ions/cm<sup>2</sup>, (d)  $2 \times 10^{16}$  ions/cm<sup>2</sup>, (e)  $5 \times 10^{16}$  ions/cm<sup>2</sup>



phases appear [34]. These are amorphous calcium phosphate, octacalcium phosphate and/or dicalcium phosphate dehydrate, and low crystalline hydroxyapatite. The application of the PIII modification with the high dose ( $2 \times 10^{16}$  ions/cm<sup>2</sup>) yielded the formation of a thinner calcium phosphate layer as seen from the intensity of the  $\nu_1$  stretching mode of PO<sub>4</sub> in spectrum 3 (Fig. 8a). The peak intensity decreased by a factor of two in comparison to the layer on the control sample and still revealed low layer crystallinity. Raman spectrum of the PTFE film (Fig. 8b, spectrum 1) was characterized by typical vibrational modes at 387.4, 576.5/598.2 (doublet), 734.1, 1216.7, 1300.5 and 1382.8 cm<sup>-1</sup> (CF<sub>2</sub> bending, C–C and C–F stretching vibrational modes, respectively [33]). The growth of the layer on the control sample from SBF (spectrum 2) hindered these features and revealed the formation of the calcium phosphate phase through the peak at 954.4 cm<sup>-1</sup> ( $\nu_1$  stretching). The  $\nu_2$  and  $\nu_4$  bending vibrations were not visible in the spectrum, and the intensity of  $\nu_1$  band was much lower (two times) than the one on the control LDPE which means that the layer grown on the control PTFE was thinner. This result was correlated with the hydrophobic behavior of the control PTFE surface which has obstructed

the layer formation. The same tendency was observed on the PTFE implanted with high dose of nitrogen ions ( $2 \times 10^{16}$  ions/cm<sup>2</sup>, spectrum 3). The peak intensity of  $\nu_1$  mode decreased four times after the modification, testifying for the effect of minimization of the calcium phosphate formation with the PIII, especially well pronounced on the treated PTFE samples.

In summary, the results showed explicitly that the modification of the LDPE and PTFE films by PIII with nitrogen ions induced topographical and chemical changes on the polymer surfaces. One explanation for the measured higher contact angle of the films implanted with the highest dose is that the implantation with the highest dose could have inserted significant changes in the polymer topography (deep and narrow rough features), which do not allow the water drop to bridge the gaps and spread well on the surfaces [35]. In addition, the highest dose treatment may have removed weakly bonded layers that may contribute to the restored hydrophobicity [36]. Good wettability is known as a prerequisite for the crystal nucleation from aqueous solutions and for the compatibility of the biomaterials with aqueous biological media [37, 38]. However, the contact angle measurement and the optical microscopy

**Fig. 5** Optical microscope images of PTFE control and plasma treated films after the calcium phosphate deposition: (a) control, (b)  $5 \times 10^{14}$  ions/cm<sup>2</sup>, (c)  $5 \times 10^{15}$  ions/cm<sup>2</sup>, (d)  $2 \times 10^{16}$  ions/cm<sup>2</sup>, (e)  $5 \times 10^{16}$  ions/cm<sup>2</sup>

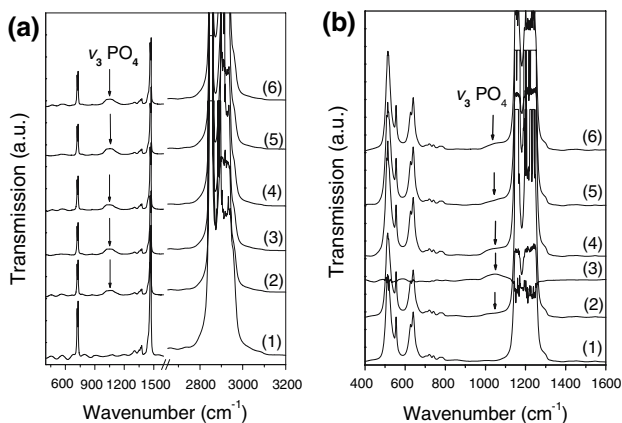
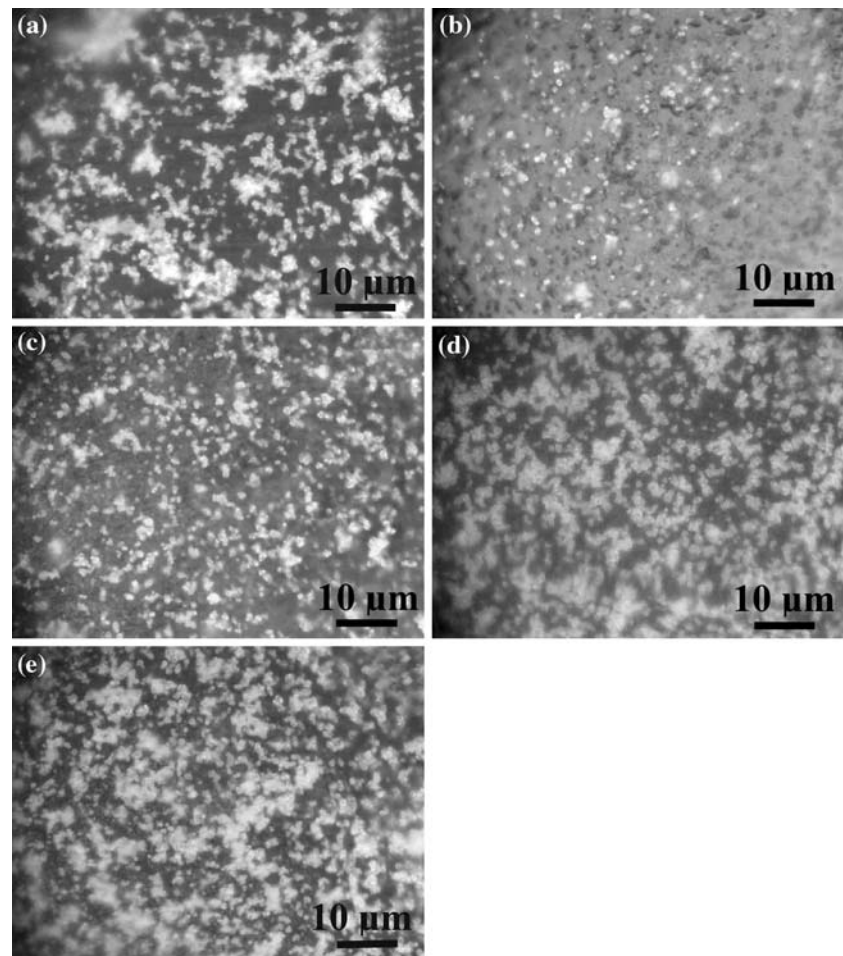


**Fig. 6** FTIR transmission spectra of (a) LDPE and (b) PTFE after PIII modification with nitrogen and immersion in SBF for 4 h: (1) control sample, (2) control with grown layer, (3)–(6) films implanted with doses of  $5 \times 10^{14}$ ,  $5 \times 10^{15}$ ,  $2 \times 10^{16}$  and  $5 \times 10^{16}$  cm<sup>-2</sup>, and with subsequently grown calcium phosphate layer

images for both polymers showed increased calcium phosphate concentration on the hydrophobic surfaces. The PIII treatment broke polymer chains and created unstable radicals. With the highest dose this effect is expected to be

stronger. Upon immersion in the SBF these surfaces could have been more reactive in respect to active species and/or water molecules in the supersaturated aqueous environment (post reaction of the free radicals) which has probably yielded the nucleation of more crystals. Our current work on the modification of 2103 and 2363 Pelletane materials, and PPG-TDI polyurethanes with PIII of nitrogen and the subsequent growth of calcium phosphate layers from SBF is expected to give more details on the observed processes.

#### 4 Conclusions

In this study, topographical and chemical changes were inserted on the surfaces of LDPE and PTFE films by PIII with nitrogen ions in order to examine their ability to induce the formation of calcium phosphate at biological conditions (from aqueous solution, resembling the blood plasma, at pH of 7.4 and 37 °C). The results obtained showed that the effect of the PIII modification on the crystal nucleation and growth of calcium phosphate from the SBF solution is ambiguous. The effect is most probably

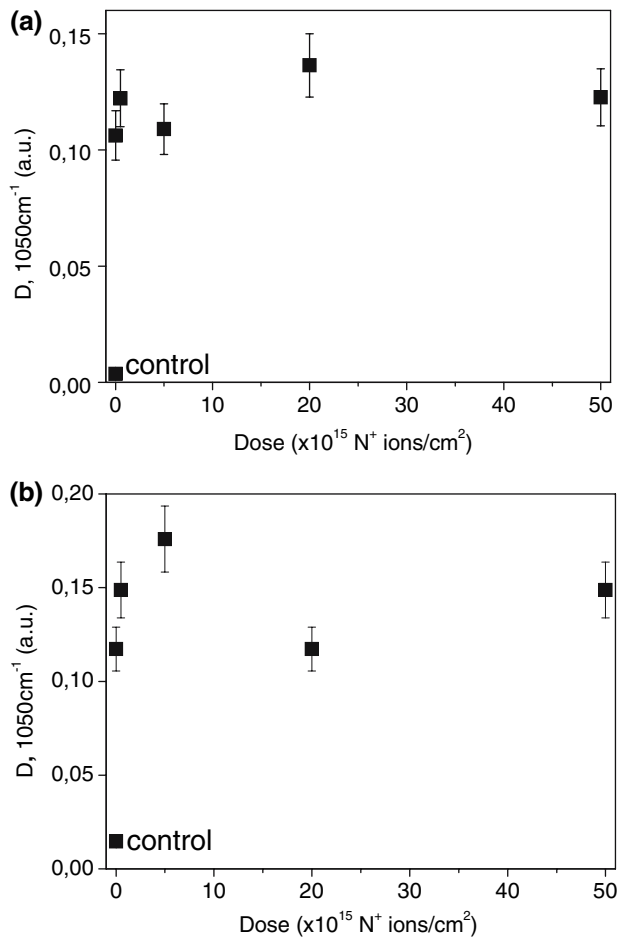


**Fig. 7** Calculation of the optical density  $D$  (relative to thickness) of the calcium phosphate layer, based on the FTIR transmission spectra at  $\nu = 1050\text{ cm}^{-1}$  for (a) LDPE and (b) PTFE films

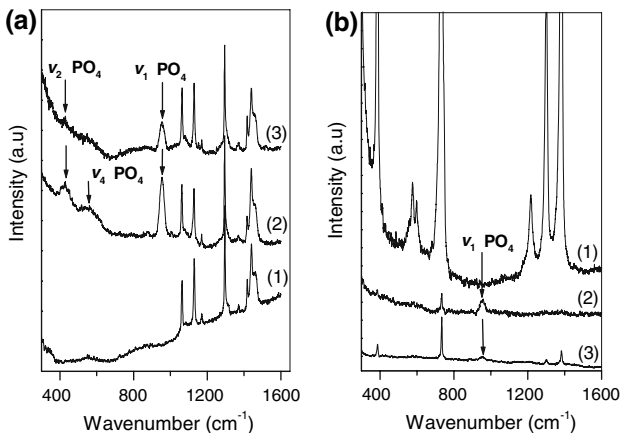


**Fig. 8** Micro-Raman spectra of (a) LDPE and (b) PTFE films: controls (spectrum 1), controls with calcium phosphate layer (spectrum 2), modified with PIII films with calcium phosphate layer (dose  $2 \times 10^{16}\text{ N}^+/\text{cm}^2$ ; spectrum 3)

based on a complex combination of surface characteristics which influences the ability of the PIII treated polymer films to induce the formation of a calcium phosphate layer.

Our current work on the PIII with nitrogen ions of two types of Pelletanes and of newly synthesized polyurethanes is expected to clarify the observed processes.

**Acknowledgements** This research was supported partly by the Bulgarian National Scientific Research Fund through Grant L1213/2002. Plasma implantation chamber at the Institute of Ion Beam Physics and Materials Research, Forschungszentrum Rossendorf, Dresden, Germany was used in the experiment.

## References

1. P. FAVIA, E. SARDELLA, R. GRISTINA and R. D'AGOSTINO, *Surf. Coat. Technol.* **169–170** (2003) 707
2. P. K. CHU, J. Y. CHEN, L. P. WANG, N. HUANG and J. JAGUR-GRODZINSKI, *e-Polymers* **012** (2003) 1
3. H. PLANK, I. SYRE, M. DAUNER and G. EGBERS, in "Polyurethanes In Biomedical Engineering", Vol ii (Elsevier, Amsterdam, 1987)
4. P. DIDISHEIM and J. WATSON, in "Biomaterials Science: An Introduction to Materials in Medicine", Edited by: B. RATNER, A. HOFFMAN, F. SCHOEN and J. LEMONS (Academic Press Inc., San Diego, CA 1996)
5. H. LEE, S. KIM and G. KHANG, in "The Biomedical Engineering Handbook", Edited by: J. BRONZINO (CRC Press, 1995) p. 581
6. P. CHUA, J. CHENA, L. WANG and N. HUANG, *Mater. Sci. Eng. R.* **36** (2002) 143
7. K. WALACHOVA, V. SVORCIK, L. BACAKOVA and V. HNATOWICZ, *Biomaterials* **23** (2002) 2989
8. C. SATRIANO, S. CARNAZZA, S. GUGLIELMINO and G. MARLETTA, *Nucl. Instrum. Methods Phys. Res. B.* **208** (2003) 287
9. D. CASTNER and B. RATNER, *Surf. Sci.* **500**(1–3) (2002) 28
10. J. ANDRADE, in "Surface and Interfacial Aspects of Biomedical Polymers", Edited by: J. ANDRADE, Vol. 2. (Plenum Press, New York, 1985)
11. J. BRASH, in "Biocompatible Polymers, Metals and Composites", Edited by: M. SZYCHER (ED) (Technomic, Lancaster, 1983)
12. P. DUCHEYNE and Q. QUI, *Biomaterials* **20** (1999) 2287
13. R. WUTHIER and J. CUMMINS, *Biochim. Biophys. Acta* **337** (1974) 50
14. H. LOWENSTAM and S. WEINER, in "On Biomineralization" (Oxford University Press, Oxford, 1989)
15. G. NANCOLLAS and W. WU, *J. Cryst. Growth* **211** (2000) 137
16. L. CAO, E. BOEVE, W. DE BRUIJN, W. ROBERTSON and F. SCHRODER, *Scan. Microsc.* **7**(3) (1993) 1049
17. M. TIRRELL, E. KOKKOLI and M. BIESALSKI, *Surf. Sci.* **500** (2002) 61
18. S. DAWIDS, in "Test Procedures for the Blood Compatibility of Biomaterials", Edited by: D. S. KLUWER (Academic Publisher, The Netherlands, 1993), p. 3
19. T. KOKUBO and H. TAKADAMA, *Biomaterials* **27** (2006) 2907
20. E. A. VOGLER, in "Wettability, Surfactant Science Series", Edited by: J. BERG and M. DEKKER, Vol 49 (New York, 1993), p 184
21. G. MESYATS, Yu. KLYACHKIN, N. GAVRILOV and A. KONDYURIN, *Vacuum* **52** (1999) 285
22. F. HYDE, M. ALBERG and K. SMITH, *J. Ind. Microbiol. Biotechnol.* **19** (1997) 142
23. J. HUNTSBERGER in "Contact Angle: Wettability and Adhesion, Advances in Chemistry Series", Edited by: R. GOULD (ACS 1964)



24. A. KONDYURIN, V. KARMANOV and R. GUENZEL, *Vacuum* **64** (2002) 105
25. J. ZHANG, X. YU, H. LI and X. LIU, *Appl. Surf. Sci.* **185** (2002) 255
26. P. C. PAINTER, M. M. COLEMAN and J. L. KOENIG, in “The Theory of Vibrational Spectroscopy and its Application to Polymeric Materials” (Wiley, New York, 1982)
27. G. MESYATS, Y. KLYACHKIN, N. GAVRILOV, V. MIZGULIN, R. YAKUSHEV and A. KONDYURIN, *Vacuum* **47**(9) (1996) 1085
28. L. PRAMATAROVA, E. PECHEVA, R. PRESKER, M. STUTZMANN, M. MAITZ and M. PHAM, *J. Optoelectr. Adv. Mater.* **7**(1) (2005) 469
29. L. PRAMATAROVA, E. PECHEVA, T. PETROV, R. PRESKER and M. STUTZMANN, *Proc. SPIE* **5830** (2005) 419
30. L. PRAMATAROVA, E. PECHEVA, D. NESHEVA, Z. LEVI, Z. ANEVA, R. PRAMATAROVA, U. BISMAYER and T. PETROV, *Phys. Stat. Sol. C* **0**(3) (2003) 1070
31. I. ALFERIEV, S. STACHELEK, Zh. LU, A. FU, T. SELLARO, J. CONNOLLY, R. BIANCO, M. SACKS and R. LEVY, *J. Biomed. Mater. Res. A* **66** (2003) 385
32. Handbook of Optics, in “Fundamentals, Techniques and Design”, Edited by: M. BASS, Vol 1 (McGRAW-HILL, Inc., 1995), p. 9.7
33. L. SOCRATES, in “Infrared Characteristic Group Frequencies” (Wiley, New York, 1980)
34. J. C. ELLIOTT, in “Structure and Chemistry of Apatites and Other Calcium Orthophosphates” (Elsevier Science, Amsterdam, 1994)
35. D. E. PACKHAM, in “1st International. Congress on Adhesion Science and Technology: Invited Papers”, Edited by: W. J. VAN OOIJ and H. R. ANDERSON Jr (VSP Publishers, Utrecht, 1998) p. 81
36. Ch. OEHR, *Nucl. Instrum. Methods Phys. Res. B* **208** (2003) 40
37. B. PAMPLIN, ed., *Crystal Growth* (Pergamon Press, 1980)
38. V. VASILETS, A. KUZNETSOV and V. SEVASTIANOV, *J. Biomed. Mater. Res. A* **69** (2004) 428